Journal of Applied Fluid Mechanics, Vol. 11, No. 3, pp. 765-777, 2018.
Available online at www.jafmonline.net, ISSN 1735-3572, EISSN 1735-3645.
DOI: 10.29252/jafm.11.03.27905

Electrothermal Convection in Dielectric Maxwellian Nanofluid Layer

V. Sharma[1†], A. Chowdhary[1] and U. Gupta[2]

[1] *Department of Mathematics and Statistics, Himachal Pradesh University, Shimla-5, India*
[2] *Dr. S.S. Bhatnagar University Institute of Chemical Engineering and Technology, Panjab University,Chandigarh-160014, India*

†*Corresponding author Email:veena_math_hpu@yahoo.com*

(Received April 23, 2017; accepted December 5, 2017)

ABSTRACT

The influence of rheological behavior on the natural convection in a dielectric nanofluid with vertical AC electric field is investigated. The rheology of the nanofluid is described by Maxwell model for calculating the shear stresses from the velocity gradients. The employed model introduces the combined effects of movement of the molecules of the fluid striking the nanoparticles, thermophoresis and electrophoresis due to embedded nanoparticles. The exact solutions of the eigen model value problem for stress-free bounding surfaces are obtained analytically using one term Galerkin method to find the thermal Rayleigh number for onset of both non-oscillatory (stationary) and oscillatory motions. It is found that the oscillatory modes are possible for both bottom and top-heavy distributions of nanoparticles. It is observed that the value of critical Rayleigh number is decreased by a substantial amount with the increase in electric field intensity, whereas role of viscoelasticity (time relaxation parameter) is to hasten the occurence of oscillatory modes appreciably. The thermal Prandtl number is found to delay the occurence of oscillatory modes. These results are also shown graphically.

Keywords: Nanofluid; Maxwell model; Brownian motion; Thermophoresis; Electric field; Stress relaxation time; Galerkin method.

NOMENCLATURE

a	dimensionless wave number
a_c	critical wave number
c_p	specific heat
d_p	nanoparticle diameter
D_B	Brownian diffusion coefficient
D_T	thermophoretic diffusion coefficient
e	coefficient of relative variations of the dielectric constant
ϵ	dielectric constant
$\vec{\mathbf{E}}$	electric field
E_o	root mean square value of the electric field
$\vec{\mathbf{f_e}}$	force of electrical origin
$\vec{\mathbf{g}}$	gravity field due to acceleration
$\mathbf{j_p}$	mass flux of the diffusing nanoparticles
k_B	Boltzman's constant
k_f	thermal conductivity of the base fluid
k_p	thermal conductivity of the nanoparticles
k_T	thermal conductivity
L_e	Lewis number
N_A	modified diffusivity ratio
N_B	modified specific heat increment
p	pressure
p_l	thermal Prandtl number
R_e	AC electric Rayleigh number
R_m	basic density Rayleigh number
R_N	concentration Rayleigh number
t	time
T	temperature
$\vec{\boldsymbol{v}}$	velocity
(x, y, z)	co-ordinates of inertial frame of reference
β	coefficient of thermal expansion
μ	viscosity
μ_b	base fluid viscosity
ρ	nanofluid density
ρ_0	nanofluid reference density
ρ_e	density of charged electrons
ρ_f	base fluid density
ρ_p	nanoparticles density
ρc	heat capacity
ϕ	nanoparticles volume fraction
φ	root mean square of the electric potential
∇^2	laplacian operator
∇_1^2	horizontal Laplacian operator
σ	growth rate

Superscripts

´	perturbed quantities

Subscripts

b	basic state
p	particle
o	lower boundary
1	upper boundary

1. INTRODUCTION

The nanotechnology has attracted many young researchers and scientists due to its unlimited growth in the modern era. Nanofluids are engineered by suspending nanoparticles in the range of 1 to 100 nm, which are first utilized by Choi (1995) in traditional heat transfer fluids such as water, biofluids, polymer solution, oil and ethylene glycol. Nanofluids are used for a wide range of applications in chemical, biological, medical, electronics engineering and in many industrial sectors due to their enhanced characteristic in thermal conductivity. Buongiorno (2006) formulated a model in which two factors Brownian motion and thermophoresis effects are incorporated, and was used by various authors or researchers to study the thermal convection in a nanofluid layer by applying various factors in saturated porous and non-porous medium. Using this model, many researchers have investigated the criteria for the onset of thermal convection. Many researchers [Kolodner (1998), Xuan and Li (2003), Jang and Choi (2004), Tzou (2008), Das and Choi (2009), Nield and Kuznetsov (2010), Bhadauria and Agarwal (2011), Yadav, *et al*. (2013)] have investigated the onset of convection under various parameters so as to study the stability of the research problems and they have found that regular fluids due to the enhancement in the thermal conductivity exhibit higher stability than nanofluids. In all the above studies, the nanofluids are assumed to be Newtonian and it has been observed that much research work has been done on the viscous nanofluids; whereas a little research work is available to investigate and study the stability criterion of rheological (non-Newtonian) nanofluids. This is due to the complexity of the rheological non-linear terms in the Navier-Stoke's equations of motion, which are not solved easily. The other reason is that the rheological fluids are not known yet in the universe. Since there is a competition within the process of thermal convection and that of rheology (viscoelasticity) due to which convection sets in through oscillatory modes rather than stationary modes. Silver[191] and Fe_3O_4[192] nanoparticles have been found in bacteria. The first viscoelastic rate type model used worldwide is proposed by Maxwell (1866) having a great storage of energy. A rheological model proposed by oldroyd was used by Malashetty *et al*. (2009 a, b) to study double diffusive instability in a viscoelastic fluid saturating a porous medium. A linear as well as the weak nonlinear stability problem was analysed by Umavathi *et al*. (2016) to study the convective transport saturating a porous medium layer in a Maxwellian nanofluid. They have presented a linear stability analysis to investigate the onset of convective transport in a rheological model described by Maxwell and saturated by porous nanofluid layer and found that stability increases with increase in Lewis number, viscosity ratio and conductivity ratio where as it decreases with increase in the nanoparticle concentration Rayleigh number and relaxation parameter. They have further analyzed the weak nonlinear stability by using truncated Fourier series and showed that heat and mass transfer increases with increase in relaxation parameter. Recently, Sharma *et al*. (2017) have derived the expression for thermal Rayleigh number for stationary modes using Galerkin-weighted residual method and found that electric fields and the modified diffusivity ratio do not have any significant role on the onset of stationary convection. They also showed that Lewis number and modified particle density increment, concentration Rayleigh number destabilize or stabilize the system under certain wave number bands.

Electro-hydrodynamics (EHD) is the mechanics which deals with the motion of flow in fluids due to externally applied electric field and generates an instability phenomenon in nanochannels. Electrohydrodynamics enhances heat transfer, microjump fabrication, electrospray mass spectrometry, electrospray nanotechnology, micro-electromechanical system and it increases the efficiency of heat transfer, which provides a new idea to the industry. The applied electric force of fluid motions is a very effective method in getting very helpful interesting results in the cooling of laptops and devices of the flight in space separately, usage to a variety of applications ranging from electrokinetic assays to electrospray ionization, made on nanoscale being used at a large scale in the present era. In dielectric liquids characterized by low values of conductivity, Maxwell equations reduce to the electroquasistatic limit. According to the theory of Landau, electric (body) force acting on dielectric liquids mainly contains Coulomb force, dielectric force and electrostrictive force. Then a dielectric (homogeneous) viscoelastic nanofluid is heated from below so as to maintain an adverse temperature gradient due to which a gradient in the electric conductivity, σ_1 and dielectrical permittivity, ϵ are produced. Then charge in the fluid is induced in the presence of an applied DC electric field and the electric relaxation time (the built free charge). When a dielectric constant is applied, the accumulated charge in the fluid and the free charge thus built varies exponentially in time with a electric relaxation time constant ϵ/σ. However, the free charge is not accumulated by applying an alternating current electric field with a frequency quiet higher than the σ/ϵ due to the quick enhancement in the movement of the charge. Due to this it is difficult to observe any effective contribution in the temperature field due to low

dielectric loss. At this stage, the mobility of the charge, varies the body force so rapidly that its effective value instead of mean value to determine motions of the fluid, is taken rather than that of fluids with extreme low viscosity. Thus the case of alternating current electric field is dominated and well manageable field on the onset of thermal convection in a layer of dielectric fluid. Nield and Kuznetsov (2010) have analysed linear stability for the onset of natural convection in a horizontal nanofluid layer. They have found that oscillatory modes are possible for the bottom heavy distribution of the nanoparticles. Further they have established that this is due to the conservation of nanoparticles coupled with the buoyancy force. Shivkumara *et al*. (2011) have investigated stability / instability of electrothermoconvection in porous / non-porous medium including various parameters for a) both stress free boundaries, b) both rigid boundaries, c) lower rigid and upper free boundaries. They have observed that the necessary conditions are independent of the applied electric field for the existence of oscillatory modes and for small Taylor number domain. The stress free boundaries are always unstable than that of other set of boundaries. This research work was reviewed extensively by Nield and Bejan (2013). Rana *et al*. (2013) have investigated steady laminar flow mixed with convection and heat transfer characteristics of Al_2O_3 numerically using Galerkin Finite Element method with volume fraction of nanoparticles ranging upto 4% and they have presented excellent validations. Later on, steady two-dimensional and mixed convection boundary layer flow of a nanofluid over a semi-infinite vertical stretching sheet has been investigated numerically by Rana *et al*. (2014) using a Galerkin Finite Element Method (FEM). They have shown that heat transfer is effectively enhanced in nanofluids and the skin friction is reduced as compared to pure water. Recently, Kalbani *et al*. (2016) have studied the problem of unsteady natural convection nanofluid having various size of nanoparticles inside an inclined square enclosure to include magnetic field. The numerical results have been obtained by using Galerkin weighted residual Finite Element Method and they have observed that the time taken to reach the steady state is influenced by the different model parameters describing the physical system.

Much research work has been carried on electrothermal instability including various physical properties of various viscous dielectric nanofluids, using different techniques. Therefore, an attempt has been made to examine theoretically and analytically the effect of rheology on the criterion for the onset of electrothermal convection in dielectric Maxwellian nanofluid layer, which is an extension of the research work by Nield and Kuznetsov (2010) for the case of stress free bounding surfaces. The Maxwell fluid model (1866) is deployed to describe the rheological behavior of the nanofluid layer of finite depth d, for the realistic stress-free boundaries. Stability is discussed analytically applying a single-term Galerkin approximation and numerical computations have been carried out using the software Mathematica Version-5.2.

2. PROBLEM FORMULATION

An infinitely extending electrically conducting layer of incompressible dielectric Maxwellian nanofluid heated from below is considered, pervaded by vertical gravity force $\vec{\mathbf{g}}(0,0,-g)$ and is confined between two parallel xy - planes at a distance of d in which temperatures at the lower and upper boundaries are assumed to be T_0 and T_1 respectively, $(T_0 > T_1)$. In addition to this nanofluid layer is subjected to a uniform vertical alternating current. The lower surface in which a reference point in an electrical circuit is taken at the lower surface against which other potentials are measured with φ as root mean square value.

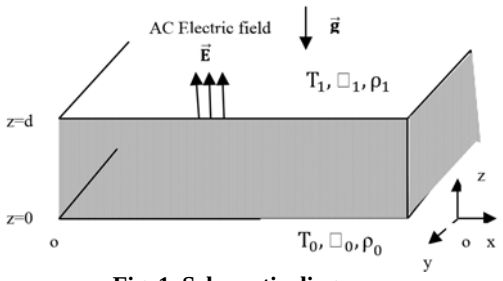

Fig. 1. Schematic diagram.

Following Buongiorno (2006) and Maxwell (1866), the continuity and momentum equations governing the physical system for the incompressible Maxwellian nanofluid are:

$$\nabla.\vec{\mathbf{v}} = 0, \tag{1}$$

$$\rho\left(1+\lambda\frac{\partial}{\partial t}\right)\left[\frac{\partial\vec{\mathbf{v}}}{\partial t}+(\vec{\mathbf{v}}.\nabla)\vec{\mathbf{v}}\right] = [-\left(1+\lambda\frac{\partial}{\partial t}\right)\left(\nabla p+\vec{\mathbf{f}_e}\right)+\left(1+\lambda\frac{\partial}{\partial t}\right)\left(\phi\rho_p+(1-\phi)\rho_0\{1-\beta(T-T_1)\}\right)\vec{\mathbf{g}}]+\mu\nabla^2\vec{\mathbf{v}}, \tag{2}$$

where $\vec{\mathbf{v}}, \mathbf{g}, \rho, p, T, \epsilon, \vec{\mathbf{E}}, \mu$ and λ denote velocity, gravitational acceleration, density, pressure, temperature, electric constant, electric field, viscosity and stress relaxation parameter (accounting for viscoelasticity), respectively and $\vec{\mathbf{f}}_e$ is the electrical origin force which is given by (Landau and Lifshitz (1960))

$$\vec{\mathbf{f}_e} = \rho_e\vec{\mathbf{E}} - \frac{1}{2}\vec{\mathbf{E}}^2\nabla\epsilon + \frac{1}{2}\nabla\left(\rho\frac{\partial\epsilon}{\partial t}\vec{\mathbf{E}}^2\right), \tag{3}$$

where ρ_e is the density of the charge. The term $\rho_e\vec{\mathbf{E}}$ is the force produced due to a free charge after the name of Coulomb and the second term $\left(-\frac{1}{2}\vec{\mathbf{E}}^2\nabla\epsilon\right)$ depends on the gradient of ϵ. The bulk of the dielectric fluid remains uninfluenced with the

electrical force $\vec{\mathbf{f}}_e$. Since the dielectric constant ϵ and the electrical conductivity σ the built up free charge is prevented for a longtime due to the sufficient relaxation appeared in the presence of electric field in most dielectric fluids at standard powerline frequencies. Thus, dielectric loss produced at these frequencies becomes very low so as to make the temperature field unchanged at the same time. Therefore, the first term $\rho_e\vec{\mathbf{E}}$, is neglected as compared to the di-electrophoretic force term $\left(-\frac{1}{2}\vec{\mathbf{E}}^2\nabla\epsilon\right)$ for most dielectric fluids. It is also assumed that the density, ρ and the dielectric constant, ϵ can be expressed as [Yadav *et al*. (2016)]

$$\rho=\rho_0\left[1-\alpha\left(T-T_0\right)\right],\epsilon=\epsilon_0\left[1-e\left(T-T_0\right)\right], \tag{4}$$

where α is the volume expansion coefficient and $e>0$ is the coefficient of the dielectric constant with temperature relative variations, which is assumed to be small. The modified pressure term using the equation

$$P=p-\frac{1}{2}\rho\frac{\partial\mathcal{E}}{\partial t}\vec{\mathbf{E}}^2. \tag{5}$$

The free charge density is assumed to be very small. The Maxwell equations by (Roberts, 1969) are :

$$\nabla.\left(\varepsilon\vec{\mathbf{E}}\right)=0, \tag{6}$$

$$\nabla\times\vec{\mathbf{E}}=0. \tag{7}$$

In view of Eq. (7), $\vec{\mathbf{E}}$ can be expressed as $\vec{\mathbf{E}}=-\nabla\varphi$ where φ is the root mean square of the electric potential.

The conservation equations for the nanoparticles are

$$\left[\frac{\partial\vec{\mathbf{v}}}{\partial t}+\left(\vec{\mathbf{v}}.\nabla\right)\vec{\mathbf{v}}\right]\phi=-\frac{1}{\rho_p}\nabla.\mathbf{j}_p. \tag{8}$$

Here ϕ is the nanoparticle volumetric fraction, ρ_p is the density of nanoparticles and $\mathbf{j}_p$ is the nanoparticles diffusion mass flux

$$\mathbf{j}_p=-\rho_pD_B\nabla\phi-\rho_p\left(\frac{D_T}{T_l}\right)\nabla T. \tag{9}$$

where D_B (Brownian diffusion coefficient) and D_T (thermophoretic diffusion coefficient) are given as

$$D_B=\frac{k_BT}{3\pi\mu_fd_p},\ D_T=\left(\frac{\mu_f}{\rho_f}\right)\left(\frac{0.26k_f}{2k_f+k_p}\right)\phi, \tag{10}$$

where k_B is Boltzman's constant, μ_f is the base fluid viscosity, d_p is the diameter of the nanoparticle, ρ_f is the base fluid density, k_f and k_p are the thermal conductivities of the base fluid and nanoparticles, respectively. Using the value of $\mathbf{j_p}$ from Eq. (9) into Eq. (8), the conservation equations of nanoparticles become as

$$\left[\frac{\partial\vec{\mathbf{v}}}{\partial t}+\left(\vec{\mathbf{v}}.\nabla\right)\vec{\mathbf{v}}\right]\phi=D_B\nabla^2\phi+\frac{D_T}{T_l}\nabla^2T. \tag{11}$$

The heat energy equation for the nanofluid is

$$\begin{aligned}\left(\rho c\right)\left[\frac{\partial\vec{\mathbf{v}}}{\partial t}+\left(\vec{\mathbf{v}}.\nabla\right)\right]T&=k_f\nabla^2T\\&+\left(\rho_pc_p\right)\left[D_B\nabla\phi.\nabla T+\frac{D_T}{T_l}\nabla T.\nabla T\right],\end{aligned} \tag{12}$$

where c_p is the specific heat of the material constituting the nanoparticles. Here both the bounding surfaces are assumed to be stress-free and the medium adjoining the nanofluid is a perfect conductor. The boundary conditions relevant to the problem are

$$w=\frac{\partial^2w}{\partial z^2}=\theta=\phi=\frac{\partial\varphi}{\partial z}=0\ at\ z=0\ and\ z=d. \tag{13}$$

3. PRIMARY FLOW

The primary flow representing the basic state is assumed to be quiescent (no settling of suspended nanoparticles) and is assumed to be stationary. Initially, no motions are present in the nanofluid flow and time-independent solutions of Eqs. (1), (2), (6), (7). (11) and (12) are taken. The temperature, nanoparticle volume fraction and pressure vary in the direction of vertical. Therefore, the solutions of the basic state satisfying Eqs. (1), (2), (6), (7), (11) and (12) are

$$\begin{aligned}&\vec{v}=\vec{v}_b=0,\ p=p_b\left(z\right),\ T=T_b\left(z\right)=T_0-\beta z,\\&\varepsilon=\varepsilon_b\left(z\right)=\varepsilon_0\left(1+e\beta z\right),\ \vec{E}=\vec{E}_b=\frac{E_0\hat{k}}{1+e\beta z},\\&\phi_b\left(z\right)=-\frac{E_0}{e\beta}\log\left(1+e\beta z\right),\end{aligned} \tag{14}$$

where subscript b denotes the steady state, $\beta=\frac{\left(T_0-T_l\right)}{d}$, is the adverse temperature gradient, $E_0=\frac{-\varphi_le\beta z}{\log\left(1+e\beta z\right)}$, is the root mean square value of the intensity of electric field at $z=0$, $\hat{k}=\hat{k}\left(0,0,1\right)$.

4. PERTURBATION EQUATIONS

Let the primary flow be slightly disturbed from the equilibrium position so as to examine the stability of the perturbed modes with respect to the involved physical variables by superimposing infinitesimal disturbances to the basic state flow. It is assumed that $\vec{\mathbf{v}}=\vec{\mathbf{v}}',p=p_b+p',\rho=\rho_b+\rho',T=T_b+T',\vec{\mathbf{E}}=\vec{\mathbf{E}}_\mathbf{b}+\vec{\mathbf{E}}',$ $\varepsilon=\varepsilon_b+\varepsilon',\phi=\phi_b+\phi',\varphi=\varphi_b+\varphi'$ where $\vec{\mathbf{v}}',\rho',p',\theta,\vec{\mathbf{E}}',$ ε',ϕ' and φ' denote the perturbations superimposed into the physical quantities of the equilibrium state.

Using these perturbations and the solutions of primary flow (14), the Eqs. (2), (7), (11) and (12) in the non-dimensional linearized perturbed form using linear theory (neglecting the products and higher orders of perturbed quantities) and Boussinesq approximation reduce to

$$\left[\nabla^4-\frac{1}{\mathrm{p_1}}\frac{\partial}{\partial \mathrm{t'}}\left(1+\lambda_1\frac{\partial}{\partial \mathrm{t'}}\right)\nabla^2\right]\mathrm{w'}+(\mathrm{R_a}\nabla_1{}^2T'+\mathrm{R_e}\nabla_1{}^2T' -\mathrm{R_N}\nabla_1{}^2\phi'-\mathrm{R_e}\frac{\partial \varphi'}{\partial \mathrm{z}})\left(1+\lambda_1\frac{\partial}{\partial \mathrm{t'}}\right)=0, \tag{15}$$

$$\frac{\partial T'}{\partial \mathrm{t'}}-\mathrm{w'}=\nabla^2T'+\frac{\mathrm{N_B}}{\mathrm{L_e}}\left(\frac{\partial T'}{\partial \mathrm{z}}-\frac{\partial \phi'}{\partial \mathrm{t'}}\right)-\frac{2\mathrm{N_A}\mathrm{N_B}}{\mathrm{L_e}}\frac{\partial T'}{\partial \mathrm{z}}, \tag{16}$$

$$\frac{\partial \phi'}{\partial \mathrm{t'}}+\mathrm{w'}=\frac{1}{\mathrm{L_e}}\nabla^2\phi'+\frac{\mathrm{N_B}}{\mathrm{L_e}}\nabla^2T', \tag{17}$$

$$\nabla^2\varphi'+\mathrm{eE_0}\frac{\partial T'}{\partial \mathrm{z}}=0\ , \tag{18}$$

where $(x,\ y,\ z)=\frac{1}{\mathrm{d}}(\mathbf{x'},\mathbf{y'},\mathbf{z'})$, $(u,\ v,\ w)\ =\frac{1}{\alpha}(\mathbf{u'},\mathbf{v'},\mathbf{w'})\mathrm{d}$, $\mathrm{t}=\frac{\mathrm{t'}}{\mathrm{d}^2}\alpha$, $\mathrm{p}=\frac{\delta \mathrm{p}}{\mu\alpha}\mathrm{d}^2$, $\phi=\frac{(\phi-\phi_0)}{(\phi_1-\phi_0)}$, $\mathrm{T}=\frac{(\mathrm{T}-\mathrm{T_1})}{(\mathrm{T_0}-\mathrm{T_1})}$, $\varphi=\mathrm{eE_0}\beta\,\mathrm{d}\varphi'$ are the non-dimensional variables and $\mathrm{p_1}=\frac{\mu}{\rho_0\alpha}$ is the thermal Prandtl number, $\mathrm{L_e}=\frac{\alpha}{\mathrm{D_B}}$ is the snanofluid Lewis number, $\mathrm{N_B}=\frac{\rho_p c_p}{\rho \mathrm{c}}(\phi_1-\phi_0)$ is the modified particle density increment, $\mathrm{N_A}=\frac{\mathrm{D_T}(\mathrm{T_0}-\mathrm{T_1})}{\mathrm{D_B}\mathrm{T_1}(\phi_1-\phi_0)}$ is the modified diffusivity ratio, $\mathrm{R_m}=\frac{\left[\rho_p\phi_0+\rho_{f0}(1-\phi_0)\right]gd^3}{\mu\alpha}$ is the basic density Rayleigh number, $\mathrm{R_N}=\frac{(\rho_p-\rho_{f0})(\phi_1-\phi_0)gd^3}{\mu\alpha}$ is the concentration Rayleigh number, $\mathrm{R_e}=\frac{\epsilon_0 e^2\mathrm{E_0}{}^2\beta^2d^2}{\mu\alpha}$ is the electric Rayleigh number, $\nabla^2=\frac{\partial}{\partial \mathrm{x}^2}+\frac{\partial}{\partial \mathrm{y}^2}+\frac{\partial}{\partial \mathrm{z}^2}$ is a Laplacian operator, $\nabla_1{}^2=\frac{\partial}{\partial \mathrm{x}^2}+\frac{\partial}{\partial \mathrm{y}^2}$ is a horizontal Laplacian operator, $\lambda_1=\frac{\lambda\alpha}{\mathrm{d}^2}$ is the non-dimensional parameter accounting for stress-relaxation time. In deriving Eq. (14) the identity $curlcurl\equiv graddiv-\nabla^2$ has been used.

5. NORMAL MODE TECHNIQUE

The partial differential Eqs. (15) - (18) are solved by using the normal mode technique by analyzing the disturbances into normal modes. The perturbed physical quantities are assumed to be of the form

$$(w',T',\phi',\varphi')=\left[W(z),\Theta(z),\Phi(z),\Psi(z)\right]\times \exp\left[\sigma t+i\left(k_x x+k_y y\right)\right], \tag{19}$$

where σ is the non-dimensional growth rate, which is generally complex in nature, k_x and k_y are the horizontal wave numbers, $\mathrm{a}=\left(k_x{}^2+k_y{}^2\right)^{\frac{1}{2}}$ is the resultant wave number . Using the expression (19), the linearized dimensionless perturbed Eqs (15) - (18) become

$$\left(D^2-a^2\right)\left[D^2-a^2-\frac{\sigma}{p_1}(1+\lambda_1\sigma)\right]W- \left[a^2\left(R_a+R_e\right)\Theta+a^2R_N\Phi+a^2R_eD\Psi\right](1+\lambda_1\sigma)=0, \tag{20}$$

$$\mathrm{W}+\left[\frac{\mathrm{N_B}}{\mathrm{L}_e}D+D^2-a^2-\frac{2\mathrm{N_A}\mathrm{N_B}}{\mathrm{L}_e}-\sigma\right]\Theta -\frac{\mathrm{N_B}}{\mathrm{L}_e}D\Psi=0, \tag{21}$$

$$W-\frac{\mathrm{N}_A}{\mathrm{L}_e}\left(D^2-a^2\right)\Theta-\left[\frac{1}{L_e}\left(D^2-a^2\right)-\sigma\right]\Phi=0, \tag{22}$$

$$\left(D^2-a^2\right)\Psi+D\Theta=0\ , \tag{23}$$

where $\mathrm{D}=\frac{d}{dz}$. The boundary conditions (13) using the expression (19) transform to

$$\mathrm{W}=D^2W=\Theta=\Phi=D\Psi=0 \text{ at } z=0 \text{ and } z=1 \tag{24}$$

The set of differential Eqs. (20) - (23) with boundary conditions (24) constituite an eigen value problem for R_a whose solutions ought to be obtained. The case of stress-free boundaries is little artificial, however it is useful to obtain an exact/analytical solution of the problem. Using single term Galerkin approximation method, exact solutions of the system of Eqs. (20) - (23) satisfying the boundary conditions (24) of lowest mode solutions of are:

$$W=W_0\sin\pi z,\Theta=\Theta_o\sin\pi z,\Phi=\Phi_o\sin\pi z, \Psi=\Psi_o\sin\pi z \tag{25}$$

where W_o,Θ_o,Φ_o and Ψ_o are constants. Substituting solutions given by (25) into Eqs. (20) - (23), and integrating each equation by parts over the range of z $(0<z<1)$ and using Boundary conditions (24), the following matrix equation is obtained:

$$\begin{bmatrix} \mathrm{J}^2+\frac{\sigma}{p_1}\mathrm{J} & -a^2(R_a+R_e)K) & a^2R_NK & 0 \\ 1 & -\mathrm{J}-\sigma & 0 & 0 \\ 1 & \frac{\mathrm{N_A J}}{\mathrm{L}_e} & \frac{\mathrm{J}}{L_e}+\sigma & 0 \\ 0 & 0 & 0 & J \end{bmatrix} \begin{bmatrix} W \\ \Theta \\ \Phi \\ \Psi \end{bmatrix} = 0. \tag{26}$$

where $\mathrm{J}=\left(\mathrm{a}^2+\pi^2\right)$ and $K=\left(1+\lambda_1\sigma\right)$

Using orthogonality, the non-trivial solution of the above matrix exists only if the thermal Rayleigh number $\mathrm{R_a}$ is as follows

$$\begin{aligned} R_a = & \frac{1}{a^2(a^2+\pi^2)(1+\sigma\lambda_1)[\frac{(a^2+\pi^2)}{L_e}+\sigma]} \\ & [-a^2R_e(a^2+\pi^2)(1+\sigma\lambda_1)[\frac{(a^2+\pi^2)}{L_e}+\sigma] \\ & -a^2R_N(a^2+\pi^2)(1+\sigma\lambda_1) \\ & [a^2+\pi^2+\sigma+\frac{a^2N_A}{L_e}+\frac{\pi^2N_A}{L_e}]+(a^2+\pi^2) \\ & (a^2+\pi^2+\sigma)[\frac{(a^2+\pi^2)}{L_e}+\sigma] \\ & [(a^2+\pi^2)^2+\frac{\sigma(a^2+\pi^2)(1+\sigma\lambda_1)}{p_1}]]. \end{aligned} \tag{27}$$

6. RESULTS

6.1 Oscillatory Modes

Since for overstability, we wish to determine the critical Rayleigh number for the onset of instability via a state of pure oscillations of increasing amplitude by putting $\sigma=i\omega\neq 0$ in the Eq. (27) and after some algebraic simplifications, we have

$$R_a=\Delta_1+i\omega\Delta_2, \tag{28}$$

where

$$\begin{aligned} \Delta_1 = & \frac{-L_ep_1R_N\left(\mathrm{a}^2+\pi^2\right)^2}{p_1\left[\left(a^2+\pi^2\right)^2+\omega^2L_e^2\right]} \\ & -\frac{\omega^4L_e^2\left(a^2+\pi^2\right)}{a^2p_1\left[\left(a^2+\pi^2\right)^2+\omega^2L_e^2\right]} \\ & +\frac{\omega^2L_e^2\left(a^2+\pi^2\right)^3}{a^2\left[\left(a^2+\pi^2\right)^2+\omega^2L_e^2\right]\left(1+\omega^2\lambda_1^2\right)} \\ & -\frac{L_e^2\omega^2\left(R_e+R_N\right)}{\left[\left(a^2+\pi^2\right)^2+\omega^2L_e^2\right]\left(1+\omega^2\lambda_1^2\right)} \end{aligned} \tag{29}$$

$$\begin{aligned} \Delta_2 = & \frac{L_eR_N\left(a^2+\pi^2\right)(-1+N_A)}{\left[\left(a^2+\pi^2\right)^2+\omega^2L_e^2\right]} \\ & +\frac{\left(a^2+\pi^2\right)^4}{a^2p_1\left[\left(a^2+\pi^2\right)^2+\omega^2L_e^2\right]} \\ & -\frac{p_1\left(-1+\left(a^2+\pi^2\right)\lambda_1\right)}{a^2p_1\left[\left(a^2+\pi^2\right)^2+\omega^2L_e^2\right]\left(1+\omega^2\lambda_1^2\right)} \\ & +\frac{\omega^2L_e^2\left(a^2+\pi^2\right)^2}{a^2p_1\left[\left(a^2+\pi^2\right)^2+\omega^2L_e^2\right]} \\ & -\frac{\omega^2L_e^2\left(a^2+\pi^2\right)^2\left[-1+\left(a^2+\pi^2\right)\lambda_1\right]}{a^2\left[\left(a^2+\pi^2\right)^2+\omega^2L_e^2\right]\left(1+\omega^2\lambda_1^2\right)} \\ & +\frac{R_NL_e^2\left(a^2+\pi^2\right)}{\left[\left(a^2+\pi^2\right)^2+\omega^2L_e^2\right]}. \end{aligned} \tag{30}$$

Since $\omega\neq 0$ for oscillatory modes, therefore, Eq. (28) implies that $\Delta_2=0$ which on simplification yields a dispersion relation as

$$\mathrm{a_1}\omega^4+\mathrm{a_2}\omega^2+\mathrm{a_3}=0, \tag{31}$$

where

$$\begin{aligned} \mathrm{a_1} = & \lambda_1^2\mathrm{L_e}\left(\mathrm{a}^2+\pi^2\right)\left[\mathrm{L_e}+2\left(\mathrm{a}^2+\pi^2\right)\right] \\ & +\lambda_1\mathrm{L_e^2}\left(\mathrm{a}^2+\pi^2\right)^2\left[1+\left(\mathrm{a}^2+\pi^2\right)\lambda_1\right], \\ \mathrm{a_2} = & \mathrm{p_1}\left(\mathrm{a}^2+\pi^2\right)^2\left[\mathrm{L_e}+\lambda_1\left(\mathrm{a}^2+\pi^2\right)\right] \\ & -\lambda_1\left[\mathrm{L_e}+\lambda_1\left(\mathrm{a}^2+\pi^2\right)\right] \\ & \left\{1-\mathrm{L_e a^2 p_1}\left(\mathrm{a}^2+\pi^2\right)^3\left(\mathrm{R_e}+\mathrm{R_N}\right)\right\} \\ & +\mathrm{L_e}\left(\mathrm{a}^2+\pi^2\right) \\ & \left\{\begin{matrix}\mathrm{a^2 p_1}\lambda_1^2\left(\mathrm{R_e}+\mathrm{N_A R_N}\right) \\ -\left(\mathrm{a}^2+\pi^2\right)^2\left[1+\lambda_1\left(\mathrm{a}^2+\pi^2\right)\right]\end{matrix}\right\}-\mathrm{L_e^2 p_1}\lambda_1 \\ & \left\{\left(\mathrm{a}^2+\pi^2\right)^3-\mathrm{a^2 R_N}\lambda_1\left[\mathrm{R_e}+\mathrm{R_N}+\left(\mathrm{a}^2+\pi^2\right)\right]\right\}, \\ \mathrm{a_3} = & \mathrm{p_1}\left(\mathrm{a}^2+\pi^2\right)\left[\mathrm{L_e}+\lambda_1\left(\mathrm{a}^2+\pi^2\right)\right] \\ & \left\{\mathrm{a^2 R_N}+\left(\mathrm{a}^2+\pi^2\right)^3-\mathrm{a^2}\left(\mathrm{R_e}+\mathrm{N_A R_N}\right)\right\} \\ & +\left(\mathrm{a}^2+\pi^2\right)^2 \\ & \left\{\left(\mathrm{a}^2+\pi^2\right)^2\left(1+\mathrm{p_1}\right)-\mathrm{a^2 p_1}\lambda_1\left(\mathrm{R_e}+\mathrm{N_A R_N}\right)\right\} \\ & +\mathrm{L_e p_1}\left(\mathrm{a}^2+\pi^2\right) \end{aligned}$$

$$\left\{\left(a^2+\pi^2\right)^3 - a^2 R_N \lambda_1 \left[R_e + R_N + \left(a^2+\pi^2\right)\right]\right\}.$$

Then, Eq. (28) with $\Delta_2 = 0$ on simplification gives the thermal Rayleigh number for oscillatory modes as

$$\begin{aligned} R_a^{osc} = & \frac{-L_e p_1 R_N \left(a^2+\pi^2\right)^2}{p_1\left[\left(a^2+\pi^2\right)^2+\omega^2 L_e^2\right]} - \frac{\omega^4 L_e^2\left(a^2+\pi^2\right)}{a^2 p_1\left[\left(a^2+\pi^2\right)^2+\omega^2 L_e^2\right]} \\ & + \frac{\omega^2 L_e^2\left(a^2+\pi^2\right)^3}{a^2\left[\left(a^2+\pi^2\right)^2+\omega^2 L_e^2\right]\left(1+\omega^2\lambda_1^2\right)} \\ & - \frac{L_e^2\omega^2\left(R_e+R_N\right)}{\left[\left(a^2+\pi^2\right)^2+\omega^2 L_e^2\right]\left(1+\omega^2\lambda_1^2\right)} \\ & + \frac{\omega^4\lambda_1 L_e^2\left(a^2+\pi^2\right)^2}{a^2\left[\left(a^2+\pi^2\right)^2+\omega^2 L_e^2\right]\left(1+\omega^2\lambda_1^2\right)} \\ & - \frac{\omega^4\lambda_1^2 L_e^2\left(R_e+R_N\right)}{\left[\left(a^2+\pi^2\right)^2+\omega^2 L_e^2\right]\left(1+\omega^2\lambda_1^2\right)} \\ & - \frac{\left(a^2+\pi^2\right)^3\omega^2}{a^2 p_1\left[\left(a^2+\pi^2\right)^2+\omega^2 L_e^2\right]} \\ & + \frac{\left(a^2+\pi^2\right)^4\left(a^2+\pi^2+\omega^2\lambda_1\right)}{a^2\left[\left(a^2+\pi^2\right)^2+\omega^2 L_e^2\right]\left(1+\omega^2\lambda_1^2\right)} \\ & - \frac{R_e\left(a^2+\pi^2\right)^4}{\left[\left(a^2+\pi^2\right)^2+\omega^2 L_e^2\right]} - \frac{N_A R_N\left(a^2+\pi^2\right)^2}{\left[\left(a^2+\pi^2\right)^2+\omega^2 L_e^2\right]}. \end{aligned} \tag{32}$$

The oscillatory neutral solutions of Eq. (32) are obtained first by the roots of Eq. (31), which is quadratic in ω^2. As ω is real for overstability and at most there may be one change of sign in Eq. (31) implying thereby at most one positive root of Eq. (31) for which the critical thermal Rayleigh number for oscillatory modes is obtained for various values of non-dimensional wave number.

6.2 Stationary Modes

The stationary modes are characterized by putting $\omega = 0$ in Eq. (27), which yields

$$R_a = \frac{\left(a^2+\pi^2\right)^3}{a^2} - R_e - R_N\left(N_A + L_e\right), \tag{33}$$

which expresses the nanofluid thermal Rayleigh number R_a for stationary convection as a function of the dimensionless wave number a, electric Rayleigh number R_e, nanofluid Lewis number L_e, modified diffusivity ratio N_A and concentration Rayleigh number R_N.

The critical dimensionless value of the wave number for the onset of instability is obtained for $\left(\frac{dR_a}{da^2}\right)_{a^2=a_c^2} = 0$, which gives $a_c = \frac{\pi}{\sqrt{2}} \cong 2.22144$.

When the electric field is not considered, then R_e(electric Rayleigh number) is zero. In the absence of the electric Rayleigh number accounting for electric field ($R_e = 0$), expression (33) reduces to

$$R_a = \frac{\left(a^2+\pi^2\right)^3}{a^2} - R_N\left(N_A + L_e\right), \tag{34}$$

which is in good agreement with the value of thermal Rayleigh number given by Nield and Kuznetsov (2010).

When the suspension of nanoparticles is not considered ($R_N = 0, N_A = 0$), the above expression further reduces to

$$R_a = \frac{\left(a^2+\pi^2\right)^3}{a^2}, \tag{35}$$

which is the earlier result by Chandrashekhar (1961).

To investigate the effects of the electric field R_e, the nanofluid Lewis number L_e, the modified diffusivity ratio N_A and the concentration Rayleigh number R_N, on the stability of stationary modes, the behavior of $\frac{dR_a}{dR_e}$, $\frac{dR_a}{dL_e}$, $\frac{dR_a}{dN_A}$ and $\frac{dR_a}{dR_N}$ have been examined analytically.

Equation (33) gives

$$\frac{dR_a}{dR_e} = -1, \tag{36}$$

which is negative implying thereby that thermal Rayleigh number decreases with increment in R_e (electric Rayleigh number).

Equation (33) further gives

$$\frac{dR_a}{dL_e} = \frac{dR_a}{dN_A} = -R_N, \tag{37}$$

which are both negative (positive) if $R_N > 0 \left(\text{or } R_N < 0\right)$ i.e. for both the cases of top-heavy or bottom heavy particles. This depicts that both the nanofluid Lewis number L_e and the modified diffusivity ratio N_A have destabilizing / stabilizing effects for positive or negative values of R_N, respectively.

Equation (33) also yields that

$$\frac{dR_a}{dR_N} = -\left(N_A + L_e\right), \tag{38}$$

which is negative if $\left(N_A + L_e\right) > 0$. Here a positive / negative N_A, (modified diffusivity ratio), indicates

that the density of nanoparticles is smaller / larger than that of the base fluid. An increase in positive/negative values of N_A advances / reduces the thermophoresis to push the lighter / heavier nanoparticles upwards, which enhances the stabilizing effects of particle distributions. Therefore, due to the addition of nanoparticles, electric field and viscoelasticity in the regular fluid, additional parameters concentration Rayleigh number (R_N), modified diffusivity ratio (N_A), electric Rayleigh number (R_e), Lewis number (L_e) are introduced in the expression for the thermal Rayleigh number, which strongly affect the stationary convection of the nanofluid layer.

To validate the numerical results obtained to calculate the critical wave number and corresponding critical Rayleigh number to discuss the stability of the system, the computed results are obtained under the limiting case of nanoparticle and electric field in Eq. (35) i.e., $R_N = 0, N_A = 0$ (see Table 1).

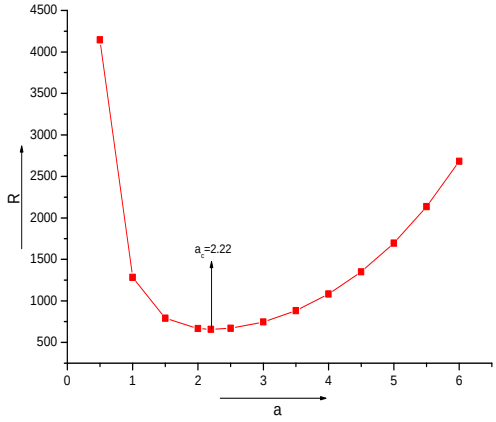

Fig. 2. Variation of thermal Rayleigh number (R_a) versus wave number (a).

Table 1 Thermal Rayleigh numbers and wave numbers of the unstable modes for stationary convection.

a	R_a^{stat}
0.5	4145.25
1	1284.23
1.5	791.194
2	667.01
2.2	657.50
2.5	670.167
3	746.528
3.5	883.478
4	1082.06
4.5	1349.34
5	1695.9
5.5	2134.74
6	2680.85

From the Table 1, it is observed that in the absence of nanoparticles and electric field, the critical thermal Rayleigh number R_a^c is equal to 657.50 and the corresponding wave number $a_c = \frac{\pi}{\sqrt{2}} \cong 2.22144$, which is the exactly same result for Rayleigh-B *é* nard instability for the ordinary fluid by Chandrasekhar (1961). Thus accuracy of the numerical method used is verified.

The expressions of thermal Rayleigh number for both stationary and oscillatory motions are presented in Eqs. (32) and (33), respectively. The variation of Rayleigh number with respect to wave-number has been plotted using Eq. (32) for oscillatory case and Eq. (33) for stationary case, whereas the experimental values and the fixed permissible values of the dimensionless parameters viz. to investigate the effects of stress-relaxation time parameter, modified diffusivity ratio, thermal Prandtl number, Lewis number, concentration Rayleigh number and electric Rayleigh number are $\lambda_1 = 0.2, p_1 = 5$, $R_N = 0.1$, $N_A = 1$, $L_e = 2000$, $R_e = 100$. The stationary thermal Rayleigh number is found to be independent of viscoelastic parameter, since it vanishes with the vanishing of ω. Thus the viscoelastic (Maxwellian) nanofluid behaves like a regular (Newtonian) nanofluid. Nield and Kuznetsov (2010) has shown the possibility of oscillatory motions to set in only for the bottom heavy nanoparticle distributions. In the present work, the work has been extended to top-heavy distribution of the nanoparticles. Equation (31) is quite complicated to find the analytical roots and to obtain critical non-dimensional wavenumbers so as to find critical thermal Rayleigh numbers for oscillatory motions, which only occur for positive values of growth rates ω. The variations of thermal Rayleigh number with respect to wavenumbers have been plotted graphically for these non-dimensional parameters for stationary cellular motion as well as for oscillatory motions. The calculation for thermofluid characteristics is based on the 10nm nanoparticles In Figs. 3a and 3b, the variation of thermal Rayleigh number R_a has been plotted versus wave number a for different values of electric Rayleigh number, R_e i.e., R_e= 0, 100, -100, 500, -500 for oscillatory and stationary motions, respectively (see Tables 2a and 2b). It is clear from the graphs that the thermal Rayleigh number takes very large values in the range of $0 < a \leq 1$ and there is no significant effect of electric Rayleigh number, R_e on thermal Rayleigh number, R_a in this regime. For $a > 1$, there is a decrease in thermal Rayleigh number with increase in electric Rayleigh number R_e implying thereby the destabilizing effect of the viscoelastic nanofluid layer for stationary as well as oscillatory modes i.e., an increase in the destabilizing electrostatic energy to the system strengthens the less stable system due to higher electric field.

The variation in the thermal Rayleigh number R_a versus wave number a for various values of the stress-relaxation parameter, λ_1 is illustrated in Fig. 4 for oscillatory motions. It is observed that the stress relaxation parameter destabilizes the oscillatory modes, since thermal Rayleigh number grow on decreasing with its varying values i.e., λ_1 = 0, 0.2,

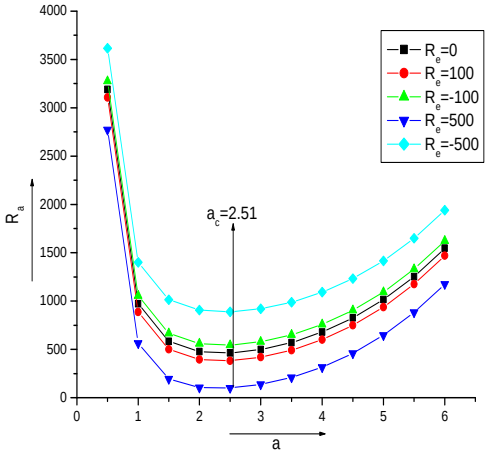

Fig. 3. (a) Variation of thermal Rayleigh number (R_a) versus wave number (a) for different values of electric Rayleigh number (R_e) for oscillatory modes.

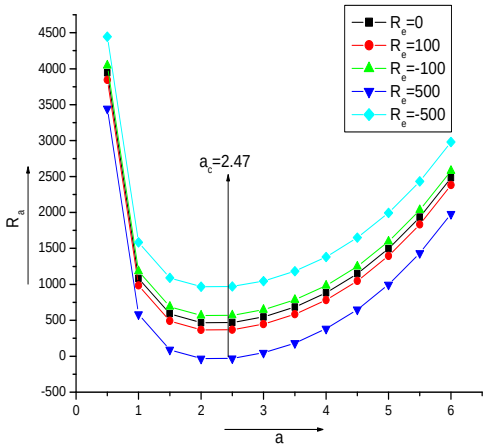

Fig. 3. (b) Variation of thermal Rayleigh number (R_a) versus wave number (a) for different values of electric Rayleigh number (R_e) for stationary convection.

Table 2 a Thermal Rayleigh numbers and wave numbers of the unstable modes for onset of oscillatory modes convection for various values of R_e= 0,100, -100, 500, -500.

a	R_a^{osc}				
	R_e=0	R_e=100	R_e=-100	R_e=500	R_e=-500
0.5	3190.11	3105.84	3274.62	2771.32	3614.95
1	971.131	887.736	1055.38	564.667	1399.47
1.5	582.754	500.546	666.516	194.325	1013.17
2	475.93	394.941	558.997	104.684	905.93
2.5	462.221	382.305	544.446	100.525	889.502
3	497.872	418.826	579.19	137.999	920.786
3.5	570.851	492.519	651.29	209.082	988.498
4	679.363	601.577	758.95	314.702	1091.41
4.5	825.786	748.471	904.623	458.502	1232.41
5	1014.86	937.946	1093.03	645.559	1416.46
5.5	1252.79	1176.24	1330.4	882.1	1649.91
6	1546.97	1470.72	1624.07	1175.4	1940.14

Table 2 b Thermal Rayleigh numbers and wave numbers of the unstable modes for onset of stationary convection for various values of R_e= 0,100, -100, 500, -500

a	R_a^{stat}				
	R_e=0	R_e=100	R_e =-100	R_e =500	R_e =-500
0.5	3945.15	3845.15	4045.15	3445.15	4445.15
1	1084.13	984.126	1184.13	584.126	1584.13
1.5	591.094	491.094	691.094	91.0942	1091.09
2	466.91	366.91	566.91	33.0898	966.91
2.5	470.067	370.067	570.067	29.9326	970.067
3	546.428	446.428	646.428	46.4279	1046.43
3.5	683.378	583.379	783.379	183.379	1183.38
4	881.955	781.955	981.955	381.955	1381.96
4.5	1149.24	1049.24	1249.24	649.245	1649.24
5	1495.8	1395.8	1595.8	995.804	1995.8
5.5	1934.64	1834.64	2034.64	1434.64	2434.64
6	2480.75	2380.75	2580.75	1980.75	2980.75

Table 3 Thermal Rayleigh numbers and wave numbers of the unstable modes for onset of oscillatory modes for various values of λ_1= 0, 0.2, 0.4, 0.6

a	R_a^{osc}			
	λ_1 =0	λ_1 =0.2	λ_1 =0.4	λ_1 =0.6
0.5	3566.59	3105.84	2079.48	1524.39
1	1045.96	887.736	576.392	407.036
1.5	613.547	500.546	313.584	211.776
2	507.77	394.941	241.029	157.822
2.5	516.41	382.305	230.91	150.16
3	592.569	418.826	253.641	166.885
3.5	726.122	492.519	301.18	202.104
4	919.144	601.577	372.317	254.976
4.5	1179.22	748.471	468.694	326.755
5	1517.16	937.946	593.465	419.819
5.5	1946.13	1176.24	750.776	537.282
6	2481.2	1470.72	945.55	682.838

0.4, 0.6 thereby advancing the onset of oscillatory convection due to the rheological behavior of the nanofluid (see Table3).

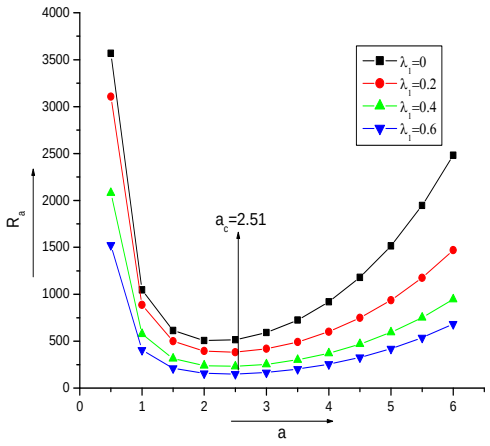

Fig. 4. Variation of thermal Rayleigh number (R_a) versus wave number (a) for different values of stress relaxation parameter (λ_1).

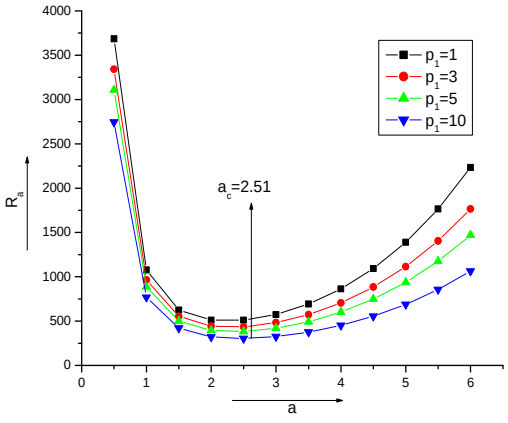

Fig. 5. Variation of thermal Rayleigh number (R_a) versus wave number (a) for different values of thermal Prandtl number (p_1).

Figure 5 depicts the effect of different values of thermal Prandtl number p_1, i.e., p_1=1, 3, 5, 10 on the thermal Rayleigh number R_a for the case of oscillatory motions against non-dimensional wave numbers. It is depicted from the figures that the thermal Rayleigh number R_a decreases with the increase in the thermal Prandtl number p_1 implying thereby advancement in the stability due to Prandtl number (see Table 4).

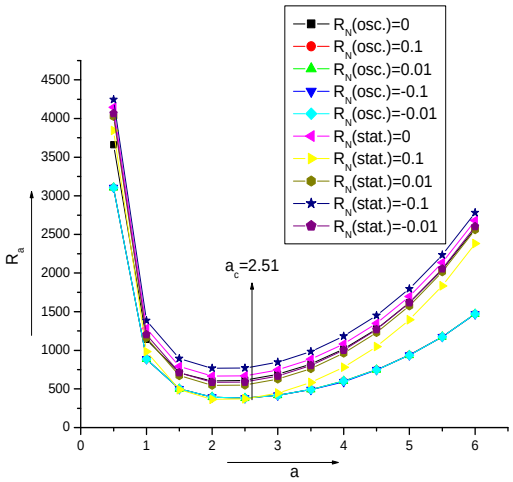

Fig. 6. Variation of thermal Rayleigh number (R_a) versus wave number (a) for different values of concentration Rayleigh number (R_N).

The thermal Rayleigh number against wave number for different values of concentration Rayleigh number i.e., R_N = 0, 0.1, 0.01, -0.1, -0.01 is plotted in Fig. 6. It is depicted that an increase in the concentration Rayleigh number R_N tends to increase the thermal Rayleigh number R_a for oscillatory motions slightly; whereas an increase in concentration Rayleigh number R_N tends to increase thermal Rayleigh number for stationary convection thereby stabilizing the physical system and the onset

Table 4 Thermal Rayleigh numbers and wave numbers of the unstable modes for onset of oscillatory modes for various values of $p_1 = 1, 3, 5$ and 10

a	R_a^{osc}			
	p_1=1	p_1=3	p_1=5	p_1=10
0.5	3684.34	3341.83	3105.84	2746.67
1	1076.05	964.965	887.736	769.178
1.5	625.626	551.977	500.546	421.174
2	510.596	442.393	394.941	322.005
2.5	510.408	434.506	382.305	303.034
3	575.192	481.947	418.826	324.519
3.5	692.83	572.571	492.519	374.91
4	863.552	705.287	601.577	451.537
4.5	1093.02	883.738	748.471	555.346
5	1389.99	1114.16	937.946	689.123
5.5	1765.35	1404.52	1176.24	856.797
6	2231.79	1764.17	1470.72	1063.14

Table 5 Thermal Rayleigh numbers and wave numbers of the unstable modes for both the onset of oscillatory modes and stationary convection for various values of RN= 0, 0.1, 001, -0.1, -0.01

a	R_a^{osc}					R_a^{stat}				
	R_N=0	R_N=0.1	R_N =0.01	R_N=-0.1	R_N=-0.01	R_N=0	R_N=0.1	R_N=0.01	R_N=-0.1	R_N=-0.01
0.5	3660.83	3105.84	3105.61	3105.32	3105.55	4145.25	3845.15	4025.24	4245.35	4065.26
1	1140.45	887.736	887.478	887.164	887.421	1284.23	984.125	1164.22	1384.33	1204.24
1.5	708.406	500.546	500.252	499.894	500.186	791.144	491.094	671.184	891.294	711.204
2	603.069	394.941	394.61	394.207	394.536	667.01	366.91	547	767.11	587.02
2.5	612.176	382.305	381.94	381.496	381.859	670.167	370.067	550.157	770.267	590.177
3	688.796	418.826	418.433	417.955	418.346	746.528	446.428	626.518	846.628	666.538
3.5	822.781	492.519	492.101	491.593	492.008	883.478	583.378	763.468	983.578	803.488
4	1016.2	601.577	601.136	591.542	601.037	1082.06	781.955	962.05	1182.16	1002.07
4.5	1276.62	748.471	748.006	747.439	747.902	1349.34	1049.24	1229.33	1449.44	1269.35
5	1614.87	937.946	937.454	936.858	937.347	1695.9	1395.8	1575.89	1796	1615.91
5.5	2044.1	1176.24	1175.72	1175.09	1175.61	2134.74	1834.64	2014.73	2234.84	2054.75
6	2579.41	1470.72	1470.18	1469.51	1470.06	2680.85	2380.75	2560.84	2780.95	2600.86

of oscillatory motion is delayed (see Table 5). Also at high thermophoretic diffusivity, thermophoresis initiates turbulence in viscoelastic nanofluids quickly and so it destabilizes the system.

In Figs. 7 and 8, the effect of various values of modified diffusivity ratio N_A i.e., 0, 20, -20, 50, -50 and Lewis number L_e i.e., 4000, 6000 (non-dimensional parameter accounting for Brownian motion D_B) on the cases of stationary and oscillatory modes have been displayed (see Tables 6 and 7). The graphs of both the figures clearly depict that the stability of the system is slightly affected due to the variations in both Lewis number and the modified diffusivity ratio.

It is also observed from all the graphs that stationary convection is the preferred manner of instability and the critical wavenumber remains same for the stationary convection (i.e., a_c=2.47) and the oscillatory motions (i.e., a_c=2.51) with respect to variations in various physical parameters.

7. CONCLUSIONS

The effect of rheological behaviour described by Maxwell model to investgate the thermal convection in an electrically conducting viscoelastic nanofluid to include an external vertical A.C electric field for stress free boundaries is studied. The characteristic value problem satisfying the appropriate boundary conditions was solved analytically using linear theory and perturbation technique followed by numerical computations. Using one term Galerkin method, an exact analytical solution is obtained and the results are encapsulated in Eq. (31) for the stationary convection and Eq. (29) for the oscillatory motion. It is established that the effect of electric field is to destabilize both stationary and oscillatory

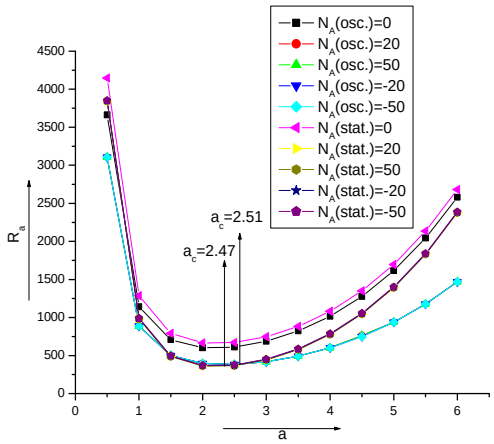

Fig. 7. Variation of thermal Rayleigh number (R_a) versus wave number (a) for different values of modified diffusivity ratio (N_A).

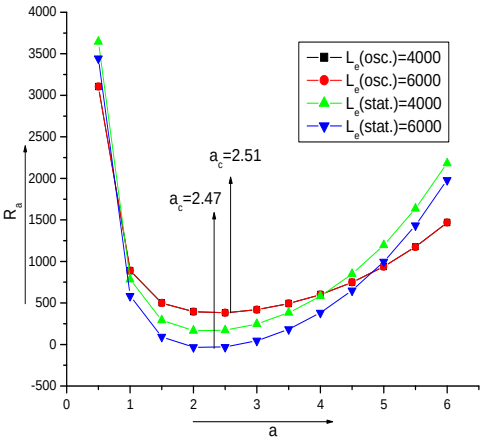

Fig. 8. Variation of thermal Rayleigh number (R_a) versus wave number (a) for different values of Lewis number (L_e).

Table 6 Thermal Rayleigh numbers and wave numbers of the unstable modes for both the onset of oscillatory modes and stationary convection for various values of N_A= 0, 20, 50, -20, -50

a	R_a^{osc}		R_a^{stat}	
	L_e=4000	L_e=6000	L_e=4000	L_e=6000
0.5	3105.41	3105.27	3645.15	3445.15
1	887.561	887.503	784.125	584.125
1.5	500.399	500.351	291.094	91.0937
2	394.781	394.781	166.91	-33.0902
2.5	382.11	382.045	170.067	-29.9329
3	418.575	418.492	246.428	46.4276
3.5	492.183	492.072	383.378	183.378
4	601.117	600.965	581.955	381.955
4.5	747.832	747.621	849.244	649.244
5	937.051	936.756	1195.8	995.803
5.5	1174.98	1174.57	1634.64	1434.64
6	1468.96	1468.38	2180.75	1980.75

Table 7 Thermal Rayleigh numbers and wave numbers of the unstable modes for both the onset of oscillatory modes and stationary convection for various values of L_e= 4000, 6000

a		R_a^{osc}					R_a^{stat}			
	N_A=0	N_A=20	N_A=50	N_A=-20	N_A=-50	N_A =0	N_A =20	N_A=50	N_A=-20	N_A=-50
0.5	3660.83	3105.84	3105.84	3105.84	3105.84	4145.25	3843.25	3840.25	3847.25	3850.25
1	1140.45	887.736	887.736	887.736	887.737	1284.23	982.225	979.225	986.225	989.225
1.5	708.406	500.545	500.545	500.546	500.547	791.194	489.194	486.194	493.194	496.194
2	603.069	394.941	394.941	394.941	394.942	667.01	365.01	362.01	369.01	372.01
2.5	612.176	382.304	382.303	382.305	382.305	670.167	368.167	365.167	372.167	375.167
3	688.796	418.826	418.825	418.827	418.827	746.528	444.528	441.528	448.528	451.528
3.5	822.781	492.518	492.517	492.519	492.52	883.478	581.478	578.478	585.478	588.478
4	1016.2	601.576	601.576	601.577	601.578	1082.06	780.055	777.055	784.055	787.055
4.5	1276.62	764.929	764.929	748.471	748.472	1349.34	1047.34	1044.34	1051.34	1054.34
5	1614.87	937.944	937.944	937.946	937.946	1695.9	1393.9	1390.9	1397.9	1400.9
5.5	2044.1	1176.23	1176.23	1176.24	1176.24	2134.74	1832.74	1829.74	1836.74	1839.74
6	2579.41	1470.72	1470.72	1470.72	1470.72	2680.85	2378.85	2375.85	2382.85	2385.85

modes. The thermal Prandtl number, p_l Lewis number, L_e and the stress relaxation parameter, λ_1 have destabilizing effects thereby increasing the region of instability for both stationary and oscillatory modes. With an increase in the concentration Rayleigh number, oscillatory frequency remains uninfluenced, whereas increase in concentration Rayleigh number R_N hasten the onset of convection, thereby stabilizing the system for the nanoparticle distribution from the top and as well as from the bottom in the base fluids. The onset of both stationary and oscillatory convection are found to be uninfluenced with the top and bottom-heavy distribution of nanoparticles.

ACKNOWLEDGEMENT

The authors gratefully acknowledge the financial support from UGC-MRP (43-435/2014(SR)) and constructive remarks of two refrees which were helpful in the improvement of the manuscript.

REFERENCES

Bhadauria, B. S. and S. Agarwal (2011). Natural convection in a nanofluid saturated rotating porous layer: a nonlinear study, *Journal of Transport in Porous Media* 87, 585–600.

Buongiorno, J. **(**2006). Convective transport in nanofluids, *ASME Journal of Heat Transfer* 128 , 240 –250.

Chandrasekhar, S. (1961). Hydrodynamic and Hydromagnetic stability *Oxford University Press*, Oxford.

Choi, S. (1995). Enhancing thermal conductivity of fluids with nanoparticles, *In:Siginer Wang, D. A., H. P. (eds.) Developments and Applications of Non-Newtonian Flows, ASME FED- 231/ MD.* 66, New York, 99–105.

Das, S. K. and S. U. S. Choi (2009). A review of heat transfer in nanofluids, *Journal of Advances in Heat Transfer* 41, 81–197.

Jang, S. P. and S. U. S. Choi (2004). Role of Brownian motion in the enhanced thermal conductivity of nanofluids, *Journal of Applied Physics Letter*, 84, 4316.

Kalbani, K. S. A., M. S. Alam and M. M. Rahman (2016). Finite element analysis of unsteady natural convective heat transfer and fluid flow of nanofluids inside a tilted square enclosure in the presence of oriented magnetic field, *American Journal of Heat and Mass Transfer* 3, 186-224.

Kolodner, P. **(**1998**).** Oscillatory convection in viscoelastic DNA suspensions, *Journal of Non-Newtonian Fluid Mechanics* 75, 167–192.

Landau, L. D. and E. M. Lifshitz (1960**).** Electrohydro dynamics of Continuous Media. *Oxford*.

Malashetty, M. S., M. Swamy and R. Heera (2009a). The onset of double convection in a binary viscoelastic fluid saturated anisotropic porous layer, *Journal of Zeitschrift für Angewandte Mathematik und Mechanik* 89, 356.

Malashetty, M. S., T. Wenchang and M. Swami (2009b). The onset of convection in a binary viscoelastic fluid saturated porous layer, *Journal of Physics of Fluids* 21, 84101.

Maxwell, J. C. (1866). On the dynamical theory of gases, *Journal of Philosophical Transactions of the Royal Society of London, 157*, 2678.

Nield, D. A. and A. Bejan (2013). *Convection in Porous Media. Springer.*

Nield, D. A. and A. V. Kuznetsov (2010**).** The onset of convection in a horizontal nanofluid layer of finite depth, *Europeon Journal of Mechanics-B/fluids* 29, 217-223.

Rana, P. and R. Bhargava (2014). Finite element solution of mixed convection flow of a nanofluid over a vertical stretching sheet with power law containing metal oxide nanoparticles , *International Journal of Applied Non-Linear Science* 1, 207-229.

Rana, P., R. Bhargava and A. O. Beg (2013). Finite element modeling of conjugate mixed convection flow of Al_2O_3-water nanofluid from an inclined slender hollow cylinder, *Journal of Physica Scripta* 87, 15.

Sharma**,** V., A. Kumar and A. Sharma (2017). Numerical investigations of electro-thermal convection in dielectric nanofluid layer, *Research Journal of Science and Technology* 9, 184-188.

Shivakumara, I. S., N. Chiu On and M. S. Nagashree, (2011). The effect to of electrothermoconvection in a rotating horizontal layer of Brinkman porous medium, *International Journal of Engineering Science* 49, 646-663.

Tzou, D. Y. (2008). Thermal instability of nanofluids in natural convection, *International Journal of Heat and Mass Transfer*, 51, 2967–2979.

Umavathi, C. J. and B. M. Mohite (2016). Convective transport in a porous medium layer saturated with a Maxwell nanofluid, *Journal of King Saud University –Engineering Sciences* 28, 56-68.

Xuan, Y. and Q. Li (2003). Investigation of convective heat transfer and flow features of nanofluids, *ASME Journal of Heat and Mass Transfer* 51, 2967-2979.

Yadav, D., R. Bhargava and G. S. Agarwal (2013). Thermal instability in a nanofluid layer with a vertical magnetic field, *Journal of Engineering Mathematics* 80, 147-164.

Yadav, D., J. Lee and H. H. Cho (2016). Electrothermal instability in a porous medium layer saturated by a dielectric nanofluid, *Journal of Applied Fluid Mechanics* 9, 2123-213.